

Yet another sample of RFGC galaxies

S. L. Parnovsky • A. S. Parnowski

© Springer-Verlag ●●●

Abstract We present a new version of a sample of galaxies from the Revised Flat Galaxy Catalogue (RFGC), which have redshift and HI line width data. We also give the parameters of the collective motion model determined upon this sample. The considered models of motion include the dipole (bulk flow), the quadrupole (cosmic shear) and the octupole components. We also considered higher-order multipoles. In all cases the obtained parameters matched the Λ CDM cosmology.

Keywords galaxies: kinematics and dynamics; galaxies: distances and redshifts; galaxies: spiral; methods: statistical

1 Introduction

The distribution of matter density is inhomogeneous in the region of the Universe, limited to about $100h^{-1}$ Mpc, which contains several superclusters and voids. A galaxy, besides the cosmological expansion, is also attracted to the regions with greater density. Due to this fact, the galaxies are involved in a large-scale collective motion on the background of Hubble expansion. Investigation of such a motion is important since it allows plotting the distribution of matter in the surrounding

region of the Universe and comparing this distribution with the distribution of luminous matter.

This is especially important due to the fact that the most serious challenges to the standard Λ CDM cosmology are posed by the inconsistencies in the estimations of the velocity of the bulk motion. The Λ CDM model estimates it at the level $\sim 250 \text{ km s}^{-1}$ at the scale $100h^{-1}$ Mpc. However, in some studies, for example Lauer & Postman (1994); Watkins et al. (2009); Feldman et al. (2010), the obtained values were larger by a factor of 2. The largest value of $416 \pm 79 \text{ km s}^{-1}$ was given by Feldman et al. (2010). Other results, including our own, give smaller values, which are consistent with the predictions of the Λ CDM cosmology.

In addition to redshifts we require independent estimations of distances to the galaxies. Since we deal only with spiral galaxies, we use the Tully-Fisher relation to determine these distances. In its common version it relates the intrinsic luminosity of a galaxy with its velocity width (the amplitude of its rotation curve). However, we use the ‘HI line width – linear diameter’ variant of the Tully-Fisher relation, which does not require photometric data. It is different from the common version and the data are also processed in a different fashion. If these two variants give similar results, this is a strong evidence of their correctness. For this reason, it is important to continue the research of the collective motions of galaxies, even if it can not boast the best accuracy or exceptionally large depth. Of course, different versions of the Tully-Fisher relation can not be regarded as independent methods, but they can potentially give very different results.

Due to large errors in determination of distances to galaxies, which are caused both by measurement errors and by the intrinsic uncertainty of the Tully-Fisher relation, it is necessary to compile large samples, and to pay special attention to the adequate processing of the data. Also, the choice of the model of the collective mo-

S. L. Parnovsky

Astronomical Observatory, Taras Shevchenko National University of Kyiv
Observatorna str. 3, 04058 Kyiv, Ukraine
tel: +380444860021, fax: +380444862191
e-mail:par@observ.univ.kiev.ua

A. S. Parnowski

Space Research Institute
prosp. Akad. Glushkova 40 build. 4/1, 03680 MSP Kyiv-187, Ukraine
tel: +380933264229, fax: +380445264124
e-mail:parnowski@ikd.kiev.ua

tion strongly affects the results. For low-depth samples it was possible to use the simple bulk motion model. However, this model is inadequate for deeper samples and more complex models should be used. These models contain higher-order multipoles and take into account additional effects.

We study these motions using the Revised Flat Galaxy Catalogue (RFGC, Karachentsev et al. 1999). It contains data about $N = 4236$ galaxies including the information on the following parameters: Right Ascension and Declination for the epochs J2000.0 and B1950.0, galactic longitude and latitude, major and minor blue and red diameters in arcminutes in the POSS-I diameter system, morphological type of the spiral galaxies according to the Hubble classification, index of the mean surface brightness (I – high, IV – very low) and some other parameters, which are not used in this article. More detailed description of the catalogue can be found in the paper (Karachentsev et al. 1999).

2 Data used

We used the sample containing 1720 RFGC galaxies. The data for 59 galaxies were rejected due to large deviations from the Tully-Fisher relation. Thus, the resulting sample contained 1661 galaxies. In addition to RFGC data we used the data on the radial velocities of the galaxies and HI line width at the 50% level. As usual, all velocities were converted to the CMB frame and HI line widths were corrected for intrinsic absorption and turbulence. The new data were taken from the SFI++ II survey (Springob et al. 2007), 3 releases of the ALFALFA survey (Giovanelli et al. 2007; Kent et al. 2008; Martin et al. 2009) and the 40ALFA survey (Haynes et al. 2011), which contains about 40% of data to enter the final version of the ALFALFA survey. Some results of RFGC galaxies observation at the Effelsberg radio telescope were taken from the papers (Mitronova et al. 2005; Kudrya et al. 2009). From all other sources only one measurement was included in this sample from the paper (Kovač et al. 2009), which contains the results of a blind survey in the Canes Venatici region. Thus, the new sample is based on much more homogeneous data than the previous one, which is an additional benefit.

As a result, we added the data about 42 new galaxies, 5 of which were later rejected. In addition, the data on a large number of galaxies, present in the previous version of the sample, were re-measured. The majority of such data featured only slight modifications with respect to the previous version. This suggests that these data are of good quality. Nevertheless, we changed the

data for 190 out of 1623 galaxies from the previous sample. For 88 galaxies the changes were minor and did not drastically affect the results. However, the data for 47 galaxies were changed significantly. This means that for these galaxies either the HI line width changed by more than 20 km s^{-1} or the radial velocity changed by more than 40 km s^{-1} , the prior being more common. The maximal change of velocity exceeded 2000 km s^{-1} and the maximal change of HI line width was 126 km s^{-1} . We will give the details of the sample construction in Section ??.

Thus, we can say that our sample has 37 added + 47 replaced = 84 essentially different data, which equals to 5% of the sample volume. This increase of the volume is smaller than in the previous versions of the sample. This is likely due to the fact that most galaxies in the field of regard of the Arecibo radio telescope were already measured and the observations in the southern hemisphere are lagging behind. The progress in the Arecibo zone can be provided by the remaining 60% of the ALFALFA survey and the improved measurements of the rejected galaxies. The greatest impact would be provided by the southern sky observations, since these are quite scarce and the addition of new data would not only increase the sample volume but also make it more uniform and symmetric.

3 Models of the collective motion

In our previous articles (Parnovsky et al. 2001; Parnovsky & Tugay 2004; Parnovsky & Parnowski 2010a, 2011) we described the models of the collective motion we used. Here we will only give two models given there. We will start from the most complex of the previously considered models, namely the DQO-model.

$$V = R + V^{dip} + V^{qua} + V^{oct} + \Delta V. \quad (1)$$

Here V is a radial velocity of the galaxy in the CMB isotropy frame, $R = Hr$ is the Hubble velocity, r is the distance to the galaxy, ΔV is a random error, V^{dip} , V^{qua} and V^{oct} are the dipole (D), quadrupole (Q) and octupole (O) components of the non-Hubble cosmic flow. They are given by the following expressions:

$$\begin{aligned} V^{dip} &= D_i n_i, \\ V^{qua} &= R Q_{ik} n_i n_k \\ &= R (q_1 (n_1^2 - n_3^2) + q_2 (n_2^2 - n_3^2) \\ &\quad + q_3 n_1 n_2 + q_4 n_1 n_3 + q_5 n_2 n_3), \\ V^{oct} &= R^2 (O_{ikl} n_i n_k n_l + P_i n_i) = R^2 (P_i n_i \\ &\quad + o_1 (3n_1 n_2^2 - n_1^3) + o_2 (3n_1 n_3^2 - n_1^3) \\ &\quad + o_3 (3n_2 n_1^2 - n_2^3) + o_4 (3n_2 n_3^2 - n_2^3) \\ &\quad + o_5 (3n_3 n_1^2 - n_3^3) + o_6 (3n_3 n_2^2 - n_3^3) \\ &\quad + o_7 n_1 n_2 n_3). \end{aligned} \quad (2)$$

Here we use Einstein's convention – summation by repeated indices. n_i are the Cartesian components of the unit vector \vec{n} towards the galaxy, connected with the galactic coordinates l and b in the following way:

$$\begin{aligned} n_1 &= n_z = \sin b, \\ n_2 &= n_x = \cos l \cos b, \\ n_3 &= n_y = \sin l \cos b. \end{aligned} \quad (3)$$

The dipole component (bulk motion) is described by the vector \vec{D} . The quadrupole component (cosmic shear) is described by the symmetrical traceless tensor \mathbf{Q} . It has 5 independent parameters q_i . The octupole component can be described by one rank 3 tensor, but we divide it into a trace characterised by vector \vec{P} and a tensor \mathbf{O} , which is antisymmetrical with respect to each pair of indices. The latter has 7 independent parameters o_i .

Hubble velocity is determined from the generalised Tully-Fisher relation in the “angular diameter – H I line width” version by the following formula

$$\begin{aligned} R &= (C_1 + C_2 B + C_3 B T + C_4 U) \frac{W}{a} \\ &+ C_5 \left(\frac{W}{a}\right)^2 + C_6 \frac{1}{a}, \end{aligned} \quad (4)$$

where W is the corrected H I line width in km s^{-1} measured at 50% of the maximum, a is the corrected major galaxies' angular diameter in arcminutes on red POSS and ESO/SERC reproductions, U is the ratio of major galaxies' angular diameters on red and blue reproductions, T is the morphological type indicator ($T = I_t - 5.35$, where I_t is Hubble type; $I_t = 5$ corresponds to type Sc), and B is the surface brightness indicator ($B = I_{SB} - 2$, where I_{SB} is the surface brightness index from RFGC; brightness decreases from I to IV). Note that the statistical significance of each term in eq. (4) is greater than 99% according to the F-test (Fisher 1954; Hudson 1964).

Thus, the DQO-model contains 24 parameters, namely 3 components of the vector \vec{D} , 6 coefficients C_i , 5 parameters q_i of the tensor \mathbf{Q} , 3 components p_i of the vector \vec{P} and 7 parameters o_i of the tensor \mathbf{O} . By rejecting V^{oct} we get a simpler DQ-model with 14 components. Further rejecting V^{qua} leads to the simplest D-model with 9 components.

In the article (Parnovsky & Parnowski 2011) on the base of the results of Kudrya & Alexandrov (2002, 2004) we also introduced relativistic models of motion based on the idea that for the homogeneous isotropic cosmological models the dependence of the velocity $V = cz$ on the angular diameter distance $R = Hr$ in the next order in R has the form

$$V = R + \gamma R^2. \quad (5)$$

The coefficient γ is expressed through the deceleration parameter q by

$$\gamma = \frac{3 + q}{2c}. \quad (6)$$

For the standard Λ CDM cosmology we have

$$q = \frac{\Omega_m}{2} - \Omega_\Lambda = -0.61, \quad (7)$$

where Ω_m and Ω_Λ are the relative densities of matter, including dark matter, and dark energy respectively. Numerical estimations are based on the results of 7-year WMAP observations (Komatsu et al. 2010). Introducing (7) into (6) we obtain

$$\gamma_0 = 3.98 \cdot 10^{-6} \text{ s km}^{-1}. \quad (8)$$

In this article we use this so-called semi-relativistic model of galaxy motion with fixed γ in the inhomogeneous space-time, which has the form

$$V_{rel} = R + V^{dip} + V^{qua} + V^{oct} + \gamma_0 R^2 + \Delta V. \quad (9)$$

The use of γ_0 mitigates the negative impact of measurement errors in the H I line widths and the angular diameters. Please refer to the articles (Parnovsky & Parnowski 2010b, 2011) for details. Since we consider the terms proportional to R^2 separately, we should remove the terms quadratic in distance from the generalised Tully-Fisher relation (4):

$$R = (C_1 + C_2 B + C_3 B T + C_4 U) \frac{W}{a} + C_5 \frac{1}{a}. \quad (10)$$

Note that all the remaining terms in this equation are inverse proportional to the angular diameter a .

It is possible to add the next two multipoles to the DQO-model by constructing the DQOX-model

$$V = R + V^{dip} + V^{qua} + V^{oct} + V^{hex} + \Delta V \quad (11)$$

and the DQOXT-model

$$V = R + V^{dip} + V^{qua} + V^{oct} + V^{hex} + V^{(32)} + \Delta V. \quad (12)$$

The velocity components corresponding to the 16-pole and the 32-pole have the form

$$\begin{aligned}
 V^{hex} &= R^3 X_{ijkl} n_i n_j n_k n_l = R^3 (x_1 n_1^4 + x_2 n_2^4 \\
 &+ x_3 n_3^4 + x_4 n_1^3 n_2 + x_5 n_1^3 n_3 + x_6 n_2^3 n_1 \\
 &+ x_7 n_2^3 n_3 + x_8 n_3^3 n_1 + x_9 n_3^3 n_2 + x_{10} n_1^2 n_2^2 \\
 &+ x_{11} n_1^2 n_3^2 + x_{12} n_3^2 n_1^2 + x_{13} n_1^2 n_2 n_3 \\
 &+ x_{14} n_2^2 n_1 n_3 + x_{15} n_3^2 n_1 n_2), \\
 V^{(32)} &= R^4 T_{ijklm} n_i n_j n_k n_l n_m = R^4 (t_1 n_1^5 \\
 &+ t_2 n_2^5 + t_3 n_3^5 + t_4 n_1^4 n_2 + t_5 n_1^4 n_3 \\
 &+ t_6 n_2^4 n_3 + t_7 n_2^4 n_1 + t_8 n_3^4 n_1 + t_9 n_3^4 n_2 \\
 &+ t_{10} n_1^3 n_2^2 + t_{11} n_1^3 n_3^2 + t_{12} n_2^3 n_3^2 \\
 &+ t_{13} n_2^3 n_1^2 + t_{14} n_3^3 n_1^2 + t_{15} n_3^3 n_2^2 \\
 &+ t_{16} n_1^3 n_2 n_3 + t_{17} n_2^3 n_3 n_1 + t_{18} n_3^3 n_1 n_2 \\
 &+ t_{19} n_1^2 n_2^2 n_3 + t_{20} n_2^2 n_3^2 n_1 + t_{21} n_3^2 n_1^2 n_2).
 \end{aligned} \tag{13}$$

However, it is more correct to introduce these multipoles to the semi-relativistic model of motion

$$V_{rel} = R + V^{dip} + V^{qua} + V^{oct} + V^{hex} + \gamma_0 R^2 + \Delta V \tag{14}$$

and

$$V_{rel} = R + V^{dip} + V^{qua} + V^{oct} + V^{hex} + V^{(32)} + \gamma_0 R^2 + \Delta V, \tag{15}$$

where R is given by the relativistic Tully-Fisher relation (10). This is due to the $C_5 \left(\frac{W}{a}\right)^2$ term in the non-relativistic Tully-Fisher relation (4), which causes different multipoles to be indistinguishable.

4 Results

We process the new sample taking into account each model of motion described above. We created subsamples with a limitation on the distance in the non-relativistic D-model $R < R_{max}$. This is the most straightforward way for limiting the sample depth. The mean distances for the two most often used subsamples with $R_{max} = 80h^{-1}$ Mpc and $R_{max} = 100h^{-1}$ Mpc are equal to $45.4h^{-1}$ Mpc and $51.5h^{-1}$ Mpc respectively. For each subsample we determined the regression coefficients using the least square method simultaneously in the Tully-Fisher relation and the model of motion. The results obtained allow estimating the quality of the sample.

The main change since the previous sample is the slightly different apex of the dipolar component. This is demonstrated in Figure 1 where the boundaries of 1σ , 2σ and 3σ confidence areas of the apices of the dipolar component are shown for 3 different samples using the D-model with $R_{max} = 100h^{-1}$ Mpc. The new sample is shown with black lines, the sample introduced in the

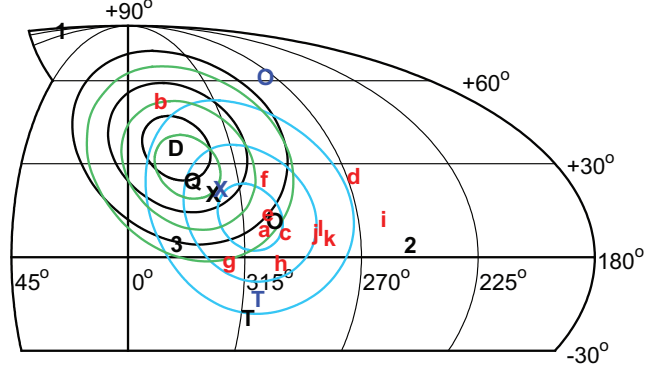


Fig. 1 A fragment of the Mollweide projection of the celestial sphere. Solid lines show the 1σ , 2σ and 3σ confidence boundaries of the bulk flow apices at $100h^{-1}$ Mpc. Black – the new sample, green – (Parnovsky & Parnowski 2010a), sky blue – (Parnovsky & Tugay 2004). The results of other authors are marked with red lowercase letters. a – (Lynden-Bell et al. 1988), b – (Lauer & Postman 1994), c – (Hudson et al. 1995), d – (Dale et al. 1999), e – (Dekel et al. 1999), f – (da Costa et al. 2000), g – (Parnovsky et al. 2001), h – (Kudrya et al. 2003), i – (Hudson et al. 2004), j – (Watkins et al. 2009), k – (Feldman et al. 2010), l – the composite sample from (Ma et al. 2011). The apices in different models are shown with uppercase letters. D – D-model, Q – DQ-model, O – DQO-model, X – DQOX model, T – DQOXT-model. For DQO-, DQOX- and DQOXT-models the non-relativistic versions are shown with black colour and the semi-relativistic – with blue colour. The numbers show the directions of the quadrupole eigenvectors in the DQO-model. 1 – maximum, 2 – intermediate, 3 – minimum.

articles (Parnovsky & Parnowski 2009, 2010a) is shown with light green lines, and the sample introduced by Parnovsky & Tugay (2004) is shown with sky blue lines. The Figure 1 is a Mollweide projection of a part of the celestial sphere.

It can be clearly seen that the apex travels in the same direction with the improvement of the sample. As a result, the apex deviated from the results of most authors (red lowercase letters in Figure 1) and became closer to the results of Lauer & Postman (1994). However, the obtained value of the bulk flow velocity 278 km s^{-1} is much smaller than that given by Lauer & Postman (1994) and is consistent with Λ CDM cosmology. Naturally, we analyzed the reasons behind this phenomenon. This change of the apex is mostly due to the improved measurements of the H I line widths of the galaxies, which were already present in the sample. All such re-measurements were double-checked by us and appeared to better match the regression relation. It is important to note that the changes in the H I line width have approximately equal probabilities to be positive or negative, thus imposing no systematic shift.

Now let us discuss the sample compilation. This step is very important, because it is one of the few manual operations in the routine. Errors at this step can lead to underestimation of the quadrupole and higher multipoles due to selection.

The new data on radial velocities V and H I line widths W were compared to the data from the previous version of the sample described by Parnovsky & Parnowski (2010a) and published in (Parnovsky & Parnowski 2009). The data about newly added galaxies were included automatically. The data, whose difference from the old ones either in V or in W was less than a few percent, were considered to be the same as before and were not changed. The data, whose difference from the old ones exceeded few percent, were considered as alternatives to the old data. Thus, we have a problem: if we have several alternative sets of data for a galaxy, which one we should choose?

We addressed this problem in the following way. In Figure 2 we plotted all the galaxies with known H I line widths. On the horizontal axis we plotted the distance according to D-model. On the vertical axis we plotted the difference between the redshift velocity and the value of the velocity following from the D-model at $R_{max} = 100h^{-1}$ Mpc. The galaxies which enter the sample are marked with dots, and the rejected galaxies – with circles. Among all possible alternatives we chose those with smallest deviations. However, this cannot be done in a straightforward way because the value of the deviation depends also on the regression parameters, which are sample-specific.

For this reason we calculated the deviations using 3 different regression relations. The first one is based on the old sample (its parameters are given in (Parnovsky & Parnowski 2010a)). The second one is based only on the galaxies, which enter the regression and have only one set of data. The third one initially includes all the candidate data, i.e. all the different sets of data for each galaxy were included as separate entries. Then we start rejecting the galaxies from the most obvious outliers. At each stage the regression relation is recalculated. However, we must stop at some point. Note that we included in the sample some galaxies with the deviations up to 3.5σ . Could we reject more galaxies and reduce the standard deviation of our sample? Let us demonstrate that this will lead to selection.

There are two effects which cause the deviation from the D-model. The first one is random scatter, which we will roughly estimate with a normal distribution with zero mean and σ^2 variance. The second one is the impact of the quadrupole and higher multipoles, which we will denote as Δ . Note that Δ greatly varies across the sample, taking the largest values at the edges of sample and in the vicinity of attractors.

Which galaxies will enter the sample and which will be rejected? If we assume the deviation from the D-model to be purely random, i.e. $\Delta = 0$, we will reject the galaxies whose deviations exceed some threshold. For the 2σ threshold the percentage of rejected galaxies is 2.3% for positive deviations and the same for negative ones. For the 2.5σ threshold these percentages are 0.6% in both ways, and for the 3σ threshold they are both less than 0.1%. Rejection of these galaxies yields no systematics.

Now let us consider a region of space where the higher multipoles account for a constant impact of $|\Delta| = \sigma$. The percentage of galaxies in such areas can be roughly estimated as 10% of the sample. A non-zero value of Δ will lead to an effective shift of the thresholds by Δ , positive for the deviations with the same sign as Δ and negative in the opposite case. This effect causes a selection which leads to an underestimation of higher multipoles. In this case the percentages of the rejected galaxies will become asymmetric. For the 2σ threshold the percentages of rejected galaxies are 15.8% in the direction of Δ and less than 0.1% in the opposite one. For the 2.5σ threshold the percentage in the direction of Δ is 6.5%, and for the 3σ threshold it becomes 2.3%. The percentages of rejects in the opposite direction for 2.5σ and 3σ thresholds are negligible. Thus, the introduced selection for this particular area is 16% for the 2σ threshold, 6.5% for the 2.5σ threshold, and 2.3% for the 3σ threshold. Multiplying this by 10% of the sample volume (about 170 galaxies), we get the expected numbers of erroneously rejected galaxies: 27 galaxies for the 2σ threshold, 11 galaxies for the 2.5σ threshold and only 4 galaxies for the 3σ threshold.

To verify these simple estimations we considered the subsamples with different deviation thresholds. They are shown in Figure 2 with horizontal lines corresponding to 2000, 2500 and 3000 km s^{-1} thresholds. Combining these thresholds with DQ- and DQO-models and 4 different limits on distance, namely $80h^{-1}$, $100h^{-1}$, $140h^{-1}$ and $170h^{-1}$ Mpc, we get 32 different combinations. For each of them we calculated the velocity of the dipolar component as well as the maximal λ_1 and the minimal λ_3 eigenvalues of the shear tensor \mathbf{Q} (the intermediate eigenvalue is not independent and is equal to $\lambda_2 = -\lambda_1 - \lambda_3$). The maximal dipolar velocity D among all possible combinations was equal to 304 km s^{-1} , which is consistent with the Λ CDM cosmology. The values of the dipolar velocity and the eigenvalues are given in Table 1. One can see that the quadrupole significantly drops with the 2500 km s^{-1} threshold for all subsamples. For the DQ-model with $R_{max} = 80h^{-1}$ Mpc subsample it drops already at the 3000 km s^{-1} threshold. The selection criterion we used

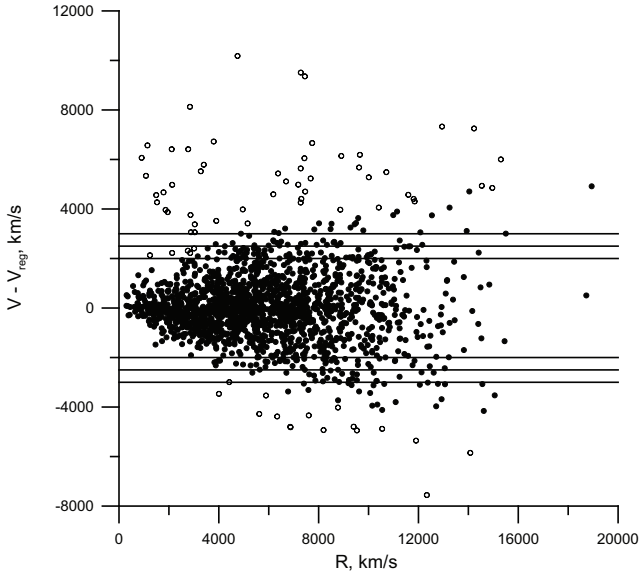


Fig. 2 The deviation from the D-model vs. the radial distance for all galaxies. Horizontal lines show the 2000, 2500 and 3000 km s^{-1} thresholds

to construct the sample appeared to be free from such problems.

We obtained the norm of the dipolar velocity component for different models and different subsamples. In Figure 3 we plotted its dependence on the sample depth R_{max} in the framework of D, DQ and DQO models. In the simplest D-model the norm grows up to the distance $100h^{-1}$ Mpc, in the DQ-model it is almost constant beyond $70h^{-1}$ Mpc, and in the DQO-model it has a minimum at about $82.5h^{-1}$ Mpc (the minimal norm is non-zero at 1.5σ confidence level). For $R_{max} > 120h^{-1}$ Mpc these values are almost constant due to the small number of more distant galaxies in our sample (47 out of 1661).

These results are obtained for unit weights of all data points. Let us see how these results will be affected by weighting. Let us choose the weights, which decrease with distance inverse proportional to $\Delta^2(R)$, where $\Delta(R)$ is a maximum deviation of the velocity from the D-model at the distance R . After calculating the norm of the dipolar velocity component for the subsamples limited at 80, 100 and $120h^{-1}$ Mpc we obtain for the D-model 243, 251, and 243 km s^{-1} respectively, for the DQ-model 245, 248, and 244 km s^{-1} , and for the DQO-model 250, 262, and 280 km s^{-1} . All these values do not differ essentially from those with unit weighting and still are consistent with Λ CDM cosmology.

Additionally, we analyzed the impact of the 16-pole and 32-pole on the velocity field. The goal of this analysis was to analyze how the inclusion of higher multipoles affects the dipole, the quadrupole and the octupole. The statistical significance of both multipoles

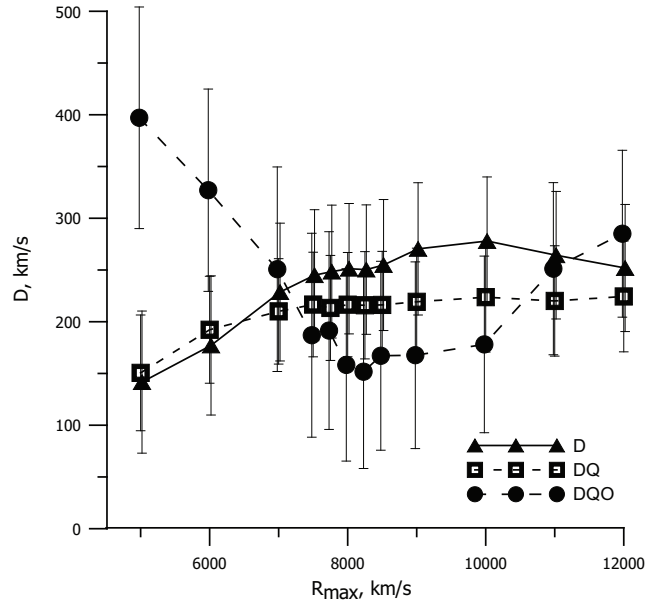


Fig. 3 The dependence of the norm of the dipolar velocity component on the sample depth R_{max} in the framework of D, DQ and DQO models

exceeds 99.9% according to F-test and the inclusion of the 16-pole reduces the RMS error by 4.5%. The semi-relativistic DQOX-model gives a much better apex as compared to the semi-relativistic DQO-model and the value of the dipolar velocity 236 km s^{-1} is also reasonable. Thus, the semi-relativistic DQOX-model can be used for deep samples. The DQOXT-model contains too much parameters and it is too early to be considered unless the sample volume and accuracy is essentially improved. The maximal dipolar velocity in these models appeared to be equal to 342 km s^{-1} in the DQOXT-model with $R_{max} = 80h^{-1}$ Mpc, which is marginally consistent with Λ CDM cosmology.

In Figure 1 we plotted the apices of the dipolar velocity in different models of motion. The letter D denotes the D-model, Q – the DQ-model, O – the DQO-model, X – the DQOX model and T – the DQOXT-model. For DQO-, DQOX- and DQOXT-models both the non-relativistic and the semi-relativistic versions are shown with black and blue colour respectively. One can see that the non-relativistic DQO-model gives the apex closest to the results of most authors. This is consistent with our earlier results (Parnovsky & Parnowski 2008, 2011) of Monte Carlo simulations, which demonstrate that the DQO-model gives the best fit to the data. However, the apex in the semi-relativistic DQO-model is way beyond all reasonable confidence boundaries. This is due to the low value of the dipolar velocity in this model, which yields large errors in the determination of the apex.

Table 1 The impact of the deviation threshold on the dipolar velocity and the maximal and minimal eigenvalues of the quadrupole

Max deviation, km s^{-1}	D , km s^{-1}				λ_1 , %				λ_3 , %			
	Full	3000	2500	2000	Full	3000	2500	2000	Full	3000	2500	2000
R_{max} , h^{-1} Mpc	DQ-model											
80	217	197	186	195	7.4	3.1	2.5	3.5	-5.8	-3.7	-4.0	-3.3
100	224	213	195	227	6.2	6.2	3.5	2.5	-4.2	-4.0	-3.3	-3.1
140	233	222	196	225	3.7	3.8	2.4	2.8	-3.9	-4.5	-3.4	-4.0
170	228	225	196	227	4.0	3.9	2.4	2.9	-4.4	-4.5	-3.4	-4.2
R_{max} , h^{-1} Mpc	DQO-model											
80	158	304	269	258	7.1	7.0	5.6	3.5	-5.6	-6.5	-6.3	-4.0
100	178	212	283	275	7.3	7.1	4.7	2.9	-4.8	-4.8	-4.4	-4.0
140	292	261	269	236	7.0	7.3	5.2	4.3	-6.5	-6.5	-5.5	-6.0
170	304	260	269	237	7.1	7.3	5.2	4.3	-6.7	-6.4	-5.5	-6.2

For reference we give the parameters of the non-relativistic DQO-model at $R_{max} = 100h^{-1}$ Mpc. The residual mean square error is $\sigma = 1112 \text{ km s}^{-1}$.

The coefficients of the generalised Tully-Fisher relation are

$$\begin{aligned}
 C_1 &= 18.0 \pm 1.3, C_2 = 1.59 \pm 1.8, \\
 C_3 &= -0.27 \pm 0.11, C_4 = 6.5 \pm 1.1, \\
 C_5 &= (-7.2 \pm 1.1) \cdot 10^{-3}, C_6 = -919 \pm 82.
 \end{aligned} \tag{16}$$

The dipolar velocity is equal to $D = 178 \text{ km s}^{-1}$ and points to the apex with the galactic coordinates $l = 303^\circ$, $b = +11^\circ$. The components of the dipolar velocity are equal to $D_z = 35 \pm 74 \text{ km s}^{-1}$, $D_x = 94 \pm 95 \text{ km s}^{-1}$, $D_y = -147 \pm 94 \text{ km s}^{-1}$. Feldman et al. (2010) using a model similar to DQO on the sample with the same depth $100h^{-1}$ Mpc obtained the dipolar velocity $D = 416 \pm 78 \text{ km s}^{-1}$ pointed towards $l = 282 \pm 11^\circ$, $b = +6 \pm 6^\circ$.

The quadrupolar component is described by its 5 irreducible components:

$$\begin{aligned}
 q_1 &= (7.2 \pm 1.5)\%, q_2 = (-2.7 \pm 1.6)\%, \\
 q_3 &= (-0.8 \pm 2.0)\%, q_4 = (1.9 \pm 2.4)\%, \\
 q_5 &= (-1.6 \pm 2.6)\%.
 \end{aligned} \tag{17}$$

It can be also represented by its eigenvalues $\lambda_1 = (7.27 \pm 1.54)\%$, $\lambda_2 = (-2.43 \pm 1.46)\%$, $\lambda_3 = (-4.84 \pm 1.47)\%$ and eigenvectors pointing respectively to $l = 118^\circ$, $b = +85^\circ$ (Canes Venatici); $l = 341^\circ$, $b = +4^\circ$ (Scorpius/Norma); and $l = 71^\circ$, $b = -4^\circ$ (Cygnus/Volans) and in the opposite directions: Sculptor, Auriga and Centaurus/Vela/Carina. The direction of the eigenvector corresponding to the maximum eigenvalue is close to the Supergalactic plane and the direction corresponding to the intermediate eigenvalue is not far from the direction towards the Great Attractor. These directions are marked in Figure 1 with

numbers 1 (maximum), 2 (intermediate) and 3 (minimum). It is interesting to compare these values with those obtained by Courtois et al. (2012), who considered a sample of 1797 galaxies within $30h^{-1}$ Mpc. Their directions of the eigenvectors demonstrated good agreement with our results for $100h^{-1}$ Mpc. However, our results for $30h^{-1}$ Mpc were in not so good agreement due to a small number of galaxies in this subsample.

The octupolar component is described by 10 irreducible components:

$$\begin{aligned}
 P_1 &= (2.2 \pm 2.1) \cdot 10^{-6} \text{ s km}^{-1}, \\
 P_2 &= (1.0 \pm 2.5) \cdot 10^{-6} \text{ s km}^{-1}, \\
 P_3 &= (0.4 \pm 3.1) \cdot 10^{-6} \text{ s km}^{-1}, \\
 o_1 &= (3.0 \pm 1.5) \cdot 10^{-6} \text{ s km}^{-1}, \\
 o_2 &= (1.0 \pm 1.8) \cdot 10^{-6} \text{ s km}^{-1}, \\
 o_3 &= (6.7 \pm 1.8) \cdot 10^{-6} \text{ s km}^{-1}, \\
 o_4 &= (-2.9 \pm 2.2) \cdot 10^{-6} \text{ s km}^{-1}, \\
 o_5 &= (5.5 \pm 2.0) \cdot 10^{-6} \text{ s km}^{-1}, \\
 o_6 &= (-2.0 \pm 2.1) \cdot 10^{-6} \text{ s km}^{-1}, \\
 o_7 &= (22.0 \pm 7.3) \cdot 10^{-6} \text{ s km}^{-1}.
 \end{aligned} \tag{18}$$

The trace vector \vec{P} , which is a part of the reduced octupole tensor and shows how the dipolar component changes with distance (Parnovsky et al. 2001), points towards the direction $l = 23^\circ$, $b = +64^\circ$ (Boötes).

In Figure 4 we plotted the radial component of the velocity field calculated in the non-relativistic DQO-model with above parameters at $R = 80h^{-1}$ Mpc. The global minimum lies in the direction opposite to the apex and the global maximum matches the direction of the maximum eigenvector of the quadrupole component. This can explain the shift of the apex in the D-model towards the latter.

Note that each multipole of order $n \geq 2$, i.e. quadrupole and higher, can be represented in a reduced form, in which the multipoles of orders $n - 2$, $n - 4$ and so

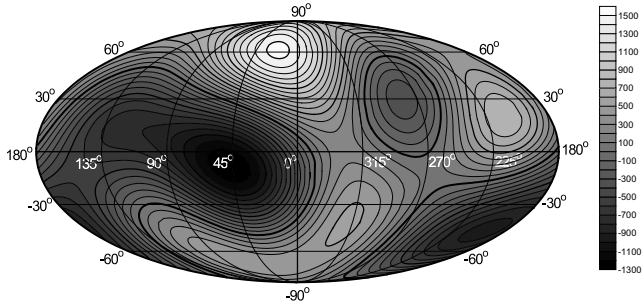


Fig. 4 The radial component of the velocity field calculated in the non-relativistic DQO-model at $R = 80h^{-1}$ Mpc

on are separated. However, it is important to realize that these lower order multipoles have the same dependence on the radial distance as the initial one. We use the reduced form for the quadrupole, separating the Hubble constant H , and for the octupole, separating the trace vector \vec{P} , which describes the change of the bulk flow velocity with distance (see (Parnovsky et al. 2001) for details). We do not use the reduced form for the 16-pole and the 32-pole, because their separated lower-order parts do not have obvious physical meaning. In addition, since these lower-order parts have a different dependence on the distance than the quadrupole and the octupole, there is no interference between them and both their reduced and full forms can be used interchangeably.

5 Conclusion

We described a new sample of RFGC galaxies intended for the study of large-scale cosmic flows. A preliminary verification with the methods described in our previous articles has shown that this new sample can be used as a basis for the study of collective motions of galaxies. We plan to modify our routine to reconstruct the distribution of matter density simultaneously with the parameters of the model of collective velocity field. In this article we applied the old routine to the new sample to verify its quality. The obtained results show principal agreement with the previous ones. It is essential that in all considered cases we obtained the values of the dipolar velocity, which are consistent with the Λ CDM cosmology. Once again, it was demonstrated that the samples with significant depth can not be considered in the framework of a simple D-model featuring only Hubble expansion and the bulk flow. For our sample with the depth $80 - 100h^{-1}$ Mpc the optimal choice is the DQO-model, which also takes into account the cosmic shear and the octupolar components. For the first time, higher-order multipoles were considered and appeared

to be statistically significant. The inclusion of the 16-pole was beneficial for the semi-relativistic model and improved the obtained results.

Acknowledgements

This research has made use of the NASA/IPAC Extragalactic Database (NED) which is operated by the Jet Propulsion Laboratory, California Institute of Technology, under contract with the National Aeronautics and Space Administration.

References

- Courtois, H. M. et al., 2012, *ApJ*, 744, 43 [arXiv:1109.3856]
da Costa, L. N. et al., 2000, *ApJ*, 537, L81
Dale, D. A. et al., 1999, *ApJ*, 510, L11
Dekel, A. et al., 1999, *ApJ*, 522, 1
Feldman, H. A. et al., 2010, *MNRAS*, 407, 2328 [arXiv:0911.5516] ■
Fisher, R. A., 1954, “Statistical methods for research workers”, Oliver and Boyd: London
Giovannelli, R. et al., 2007, *AJ*, 133, 2569 (astro-ph/0702316)
Haynes, M. P. et al., 2011, *AJ*, 142, 170 [arXiv:1109.0027]
Hudson, D. J., 1964, “Statistics Lectures on Elementary Statistics and Probability”, CERN: Geneva
Hudson, M. J. et al., 1995, *MNRAS*, 274, 305
Hudson, M. J. et al., 2004, *MNRAS*, 352, 61
Karachentsev, I. D. et al., 1999, *Bull. SAO*, 47, 5 (astro-ph/0305566)
Kent, B. R. et al., 2008, *AJ*, 136, 713 [arXiv:0806.3237]
Komatsu, E. et al., 2010, preprint [arXiv:1001.4538]
Kovač, K. et al., 2009, *MNRAS*, 400, 743 [arXiv:0904.2775]
Kudrya, Yu. N., Alexandrov, A. N., 2002, *J. Phys. Studies*, 6, 472 (in Ukrainian)
Kudrya, Yu. N., Alexandrov, A. N., 2004, *Herald Kyiv Univ. Astron.*, 39-40, 130 (in Ukrainian)
Kudrya, Yu. N. et al., 2003, *A&A*, 407, 889
Kudrya, Yu. N. et al., 2009, *Astrophysics*, 52, 335 [arXiv:0811.3690] ■
Lauer, T. R., Postman, M., 1994, *ApJ*, 425, 418
Lynden-Bell, D. et al., 1988, *ApJ*, 326, 19
Ma, Y. Z. et al., 2011, *Phys. Rev. D*, 83, 103002 [arXiv:1010.4276] ■
Martin, A. M. et al., 2009, *ApJS*, 183, 214 [arXiv:0906.2181]
Mitronova et al., 2005, *Astr. Lett.*, 31, 501 (astro-ph/0510248) ■
Parnovsky, S. L., Tugay, A. V., 2004, *Astron. Lett.*, 30, 357
Parnovsky, S. L., Parnowski A. S., 2008, *AN*, 329, 864
Parnovsky, S. L., Parnowski, A. S., 2009, preprint [arXiv:0911.3102] ■
Parnovsky, S. L., Parnowski A. S., 2010a, *Ap&SS*, 325, 163 [arXiv:0910.4640]
Parnovsky, S. L., Parnowski A. S., 2010b, *J. Phys. Studies*, 14, 3900.
Parnovsky, S. L., Parnowski A. S., 2011, *Ap&SS*, 331, 429 [arXiv:1004.4344]
Parnovsky, S. L. et al., 2001, *Astron. Lett.*, 27, 765
Springob, C. M. et al., 2007, *ApJS*, 172, 599
Watkins, R. et al., 2009, *MNRAS*, 392, 743